Journal of Alloys and Compounds 896 (2022) 163074

Contents lists available at ScienceDirect

Journal of Alloys and Compounds

journal homepage: www.elsevier.com/locate/jalcom

Low temperature magnetic study and first principle calculation in 'Mo' doped $CoFe_2O_4$ for magnetic information storage applications

Manish Kumar[a,*], Arvind Kumar[a], Abhishek Singh[b], Avneesh Anshul[c], Subhash Sharma[d], Prakash Chandra Sati[e]

[a] Experimental Research Laboratory, Department of Physics, ARSD College, University of Delhi, New Delhi, 110021, India
[b] Central Instrument Facility, Indian Institute of Technology (Banaras Hindu University), Varanasi, 221005, India
[c] CSIR-National Environmental Engineering Research Institute (NEERI), Nagpur, 440020, India
[d] CONACyT, Centro de Nanociencias y Nanotecnología. Universidad Nacional Autónoma de México, Km 107 Carretera Tijuana-Ensenada s/n, Ensenada, B.C. C.P. 22800, Mexico
[e] Department of Physics, Rajiv Gandhi Government (Post Graduate) College, Mandsaur, Madhya Pradesh, 458001, India

ARTICLE INFO

Article history:
Received 11 September 2021
Received in revised form 27 November 2021
Accepted 30 November 2021
Available online 1 December 2021

Keywords:
Rietveld refinement
Magnetism
DFT calculation
Memory applications

ABSTRACT

Structural and low temperature magnetic properties of $CoFe_{2-x}Mo_xO_4$ (x = 0.01, 0.03 and 0.05) were studied in the present work. Rietveld refinement of XRD patterns of $CoFe_{2-x}Mo_xO_4$ (x = 0.01, 0.03 and 0.05) confirm the pure phase cubic crystal structure in *Fd3m* space group. The decrease in lattice parameters (a contraction of the lattice) has been observed with doping, which confirms the probability of substitution of 'Mo' at the octahedral site of parental $CoFe_2O_4$ (CFO). The micro-strain via W-H plots was found to be enhanced for $CoFe_{1.95}Mo_{0.05}O_4$ (CMFO5) sample which confirms the incorporation of 'Mo' atoms at Fe-site and subsequently reducing impurities as observed from refined patterns. The low temperature (2K) magnetic parameters were found to be greatly enhanced with 'Mo' substitution. We observed the decrease in anisotropy constant of Co^{2+} ions with 'Mo' doping and Mo^{6+} ions concentration at the tetrahedral site of CFO, increases the magnetization of the samples. Both M-H and ZFC-FC measurements confirm the ferrimagnetic behavior of all the samples. The maximum value of information storage parameter 'S' achieved around 0.442 for x = 0.03 sample at 2K. The structural parameters, electronic (density of states and band structure) and magnetic properties of pure CFO have also been investigated via computational first principle based density functional theory (DFT) calculations. The computational results are in good agreement with the experimental outputs.

1. Introduction

The emphasis of current research focuses on the magnetic materials due to their essential role in high-density information storage for memory applications, microwave absorption, energy storage devices or materials with high magnetization and switchability [1,2]. Magnetic information storage in magnetic materials is a form of non-volatile storage i.e., the information does not vanish once the storage device is not powered a distinction to volatile storage, which needs a continuous power supply, otherwise storage information/data lost [2,3]. The magnetic hysteresis (M vs. H) is liable for the use of magnetic materials as digital magnetic memory devices, meanwhile the up or positive state of the magnetization could signify a binary number '1' and the down or negative state could signify a binary number '0' [4]. Also, these states can be steady even in zero applied fields. In the case of digital "saturation" storage, the perfect written design is an arrangement of whole magnetization reversals in between positive and negative saturation values of the magnetization hysteresis curve. The attainable density of magnetic data storage depends on the acuity of these magnetization changes. The high density recording can be achieved in smaller size particles and needs stability against demagnetization due to temperature, stress, atmospheric corrosion, and oxidation. To avoid storage data loss because of the mechanical stress, we need to use the magnetic anisotropy modes during the operation [5,6]. So, for information storage devices, magnetic ferrites exhibit extraordinary physical properties that are fairly motivating for the scientific and technological applications.

Among various ferrites, ferrimagnetic spinel ferrite structure (AB_2O_4, A-tetrahedral, and B-octahedral sublattices) $CoFe_2O_4$ (CFO)

* Corresponding author.
E-mail address: mkumar2@arsd.du.ac.in (M. Kumar).

https://doi.org/10.1016/j.jallcom.2021.163074
0925-8388/

has been most widely considered material which has an extensive diversity of applications including information storage devices [7]. The electrical and magnetic properties of CFO depend on the cationic distribution in the 'A′ and 'B′ sublattices. The replacements at the 'Fe' sites of CFO by various cations like Ga, Mn, Mo, etc., have exposed pronounced potentiality of the doping for inducing magnetic and multiferroic properties [8–11].

There are very few reports available on the 'Mo' doped CFO such as Dwivedi et al. reported the evidence of ferroelectricity by the doping of 'Mo' in to CFO and claimed the simultaneous existence of the magnetic as well as ferroelectric ordering including giant dielectric constant [11]. Oroczco et al. reported 'Mo' doped CFO synthesized via conventional solid state reaction route and study the effect of doping on to the structural and magnetic properties [14]. They have concluded that the structural, magnetic and microstructural properties can be tune with the 'Mo' doping in to the CFO. Khan et al. have analyzed the 'Mo' doping in to the CFO at Fe site and confirmed the enhancement in structural, magnetic and magnetocaloric properties [18]. 'Mo' doped CFO nanoparticles have also been investigated by Heiba et al. and explained the structural and magnetic properties related with the cation distribution [13].

In the present study, the 'Fe' site of CFO is partially substituted by 'Mo' because of its considerably exciting high valence state '+6' and d^0-ness electronic configuration. The motivation behind this partial substitution of Fe^{3+} by Mo^{6+} in CFO must induce electron doping, and subsequently, the amount of Fe^{2+} ions should increase in the tetrahedral sites. Moreover, Fe^{3+} by Mo^{6+} and the d^0-ness electronic configuration are responsible for the improvement in the magnetic as well as the ferroelectric nature of CFO. Hence, ferroelectric 'Mo' modification in CFO may induce improved magnetization under the impression of information storage applications and multiferroicity in these compositions. Apart from the experimental investigations, we have also optimized our structural and magnetic experimental parameters of pure CFO with the computational first principal DFT calculation for better understanding of the base material.

2. Experimental procedure

The solid state reaction method is used to synthesize 'Mo' modified $CoFe_2O_4$ samples in the air environment with compositions $CoFe_{2-x}Mo_xO_4$ (x = 0.00, 0.01, 0.03 and 0.05), designated as CFO, CFMO1, CFMO3 and CFMO5 [11,12]. The proper stoichiometric quantities of Co_3O_4, Fe_2O_3, and MoO_3 were mixed and ground. The ground mixtures were calcined at 1050 °C for 11 h and followed by sintering at 1200 °C for 48 h with a cooling rate of 5°/min. After making the pellets of grounded calcined power with intermediate grindings, the structural measurement was done by powder X-ray diffractometer (XRD) employing Cu-K_α radiations and fitted the data by Rietveld refinement using FullProf method. The direct current (dc) magnetization M vs. H and zero field cooled-field cooled (ZFC-FC) measurements were carried out by superconducting quantum interference device magnetometer (Quantum Design MPMS XL-7) at 2–300 K.

3. Results and discussion

3.1. Structural investigations

The structural analysis has been done using powder XRD data and shown in the Fig. 1. Powder XRD pattern of pure CFO is shown in the Fig. 1(a) and confirms clear phase formation as per the previously reported data [11,13,14,18]. Powder XRD patterns with Rietveld refined data of the 'Mo' doped samples are shown in the Fig. 1(b). All experimental peaks were matched with a cubic crystal structure in the *Fd3m* space group. The lattice parameters of samples were calculated using Rietveld analysis, enlisted in Table 1. The

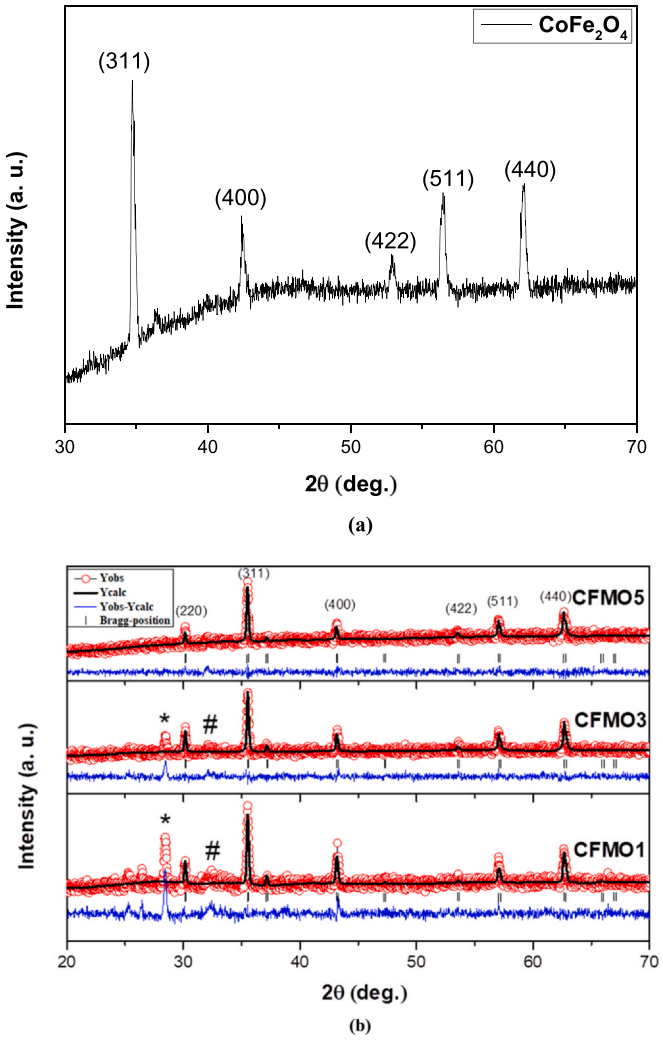

Fig. 1. (a) Powder XRD pattern of pure $CoFe_2O_4$ sample for reference and, (b) Rietveld refined XRD patterns of $CoFe_{2-x}Mo_xO_4$ ceramic samples.

calculated lattice parameters decrease (minimal amount) with increasing concentration of Mo^{6+} (r_{Mo}^{6+}) dopant ions at tetrahedral A site of the CFO spinel structure and also maintain the charge neutrality with transfer Fe^{3+} ($r_{Fe}^{3+0.645A^0}$) to Fe^{2+} ($r_{Fe}^{2+0.77A^0}$). The strain produced by the substitution of ions in the material gets relaxed by the migration of Fe^{2+} and Fe^{3+} ions. Due to this structural modification, the lattice parameters also confirm the contraction of the lattice and the probability of substitution of dopant at the tetrahedral site [11,13,14]. As, it is a well-known fact that the criteria for quality of best fit are the low values of χ^2 (1.165, 1.355 and 1.240) and straightness of the differential spectra. In the present case, the differential spectra and the values of χ^2 are indicating the best fit in these samples. We have used Wyckoff position 8a (1/2,1/2,1/2), 16d (0.125,0.125,0.125) and 32e (0.2583, 0.2583, 0.2583) for iron, cobalt and oxygen ions, respectively.

The Williamson- Hall plots for all samples are shown in Fig. 2. The micro-strain (ε) was calculated to be 9.145E-4, 7.27487E-4, and 1.05E-3 for samples CMFO1, CMFO3 and CMFO5, respectively via the slop of plot ($\beta\cos\theta$) vs. ($4\sin\theta$) as shown in Fig. 2. In addition, crystallite size was also estimated to be 61, 56, 66 nm respectively for samples CMFO1, CMFO3 and CMFO5, respectively using W-H plot. The micro-strain was found to be enhanced for CMFO5, confirming the incorporation of Mo atoms at Fe-site and subsequently reducing impurities as observed from refined patterns (shown in Fig. 1)

Table 1
Refined structural parameters (crystal structure, lattice parameters and R-factors (%)) of $CoFe_{2-x}Mo_xO_4$ ceramics including computational structural parameters of pure CFO.

Sample	Crystal Structure	Lattice parameters	R-factors (%)
CFO	Cubic ($F\,d\,3\,m$)	Theoretical: a = b = c = 8.549 Å, V = 624.88 Å^3 Experimental: a = b = c = 8.56 Å, V = 627.22 Å^3	
CFMO1	Cubic ($F\,d\,3\,m$)	a = b = c = 8.3849 Å, V = 589.53 Å^3	R_p = 4.98, R_{wp} = 6.26, R_{Bragg} = 11.4, R_f = 12.6
CFMO3	Cubic ($F\,d\,3\,m$)	a = b = c = 8.3810 Å, V = 588.70 Å^3	R_p = 4.90, R_{wp} = 6.27, R_{Bragg} = 20.1, R_f = 16.0
CFMO5	Cubic ($F\,d\,3\,m$)	a =b=c= 8.3795 Å, V = 588.36 Å^3	R_p = 4.55, R_{wp} = 5.73, R_{Bragg} = 12.9, R_f = 12.4

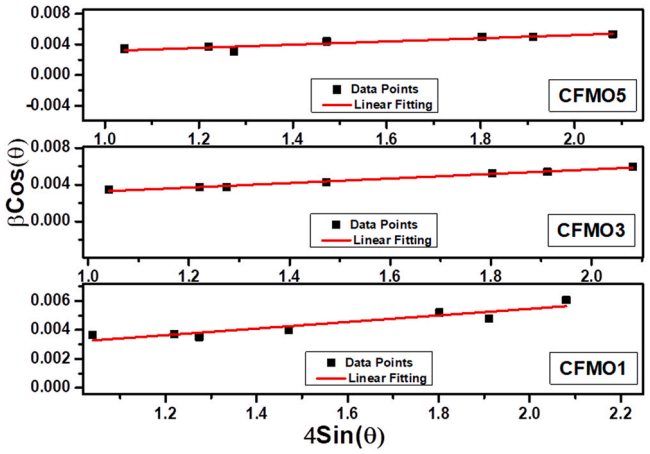

Fig. 2. W-H plots of $CoFe_{2-x}Mo_xO_4$ ceramic samples.

indicated by '*' and '#'. All the refined parameters i.e., structural, lattice parameters and R-fator (%) are tabulated in the Table 1.

3.2. Low temperature magnetic investigations

The magnetic hysteresis loop (M vs. H) of $CoFe_{2-x}Mo_xO_4$ (x = 0.01, 0.03, 0.05) samples at room temperature (300 K) and low temperature (2 K) are shown in Fig. 3(a-b). The room temperature remnant magnetization (M_r), saturation magnetization (M_s) and coercive field (H_c) values lie within the range of 3.35–4.73 emu/g, 64.89–81.62 emu/g and 156.18–179.29 Oe, respectively for x = 0.01–0.05 samples, respectively and also enlisted in Table 2. With the increase of magnetic field strength, magnetization increases monotonically and saturates at the magnetic field of 30 kOe. This indicates their ferrimagnetic behavior [14]. But at low temperature (2 K), the broadening in magnetic loops is observed with enhanced values of M_r, M_s, and H_c in the range of 25.68–37.49 emu/g, 70.46–84.52 emu/g, 1397–1439 Oe respectively for x = 0.01–0.05 samples, respectively. Such a strong temperature-dependent

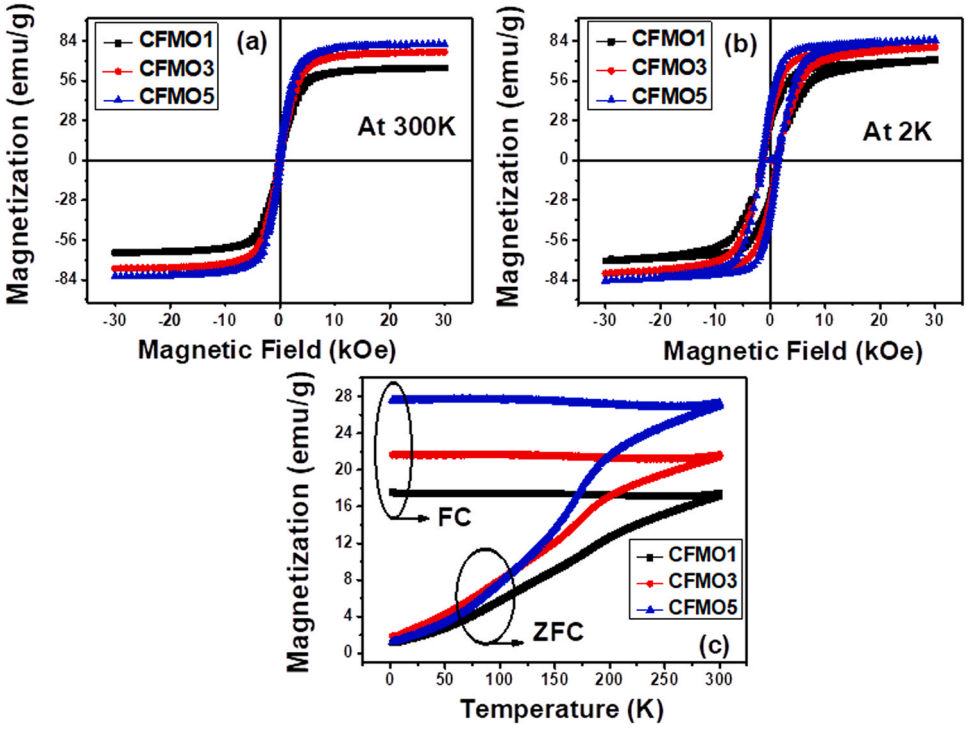

Fig. 3. (a) M-H data at 300 K, (b) M-H data at 2 K and (c) ZFC-FC data at 100 Oe, of $CoFe_{2-x}Mo_xO_4$ ceramics.

Table 2
Structural and magnetic parameters (remenancy-M_r, coercivity-H_c, saturation magnetization-M_s and remanent squareness-S at 2 K and 300 K) of CFMO1, CFMO3 and CFMO5 ceramics.

Composition (x)	Magnetic parameters at 300 K				Magnetic parameters at 2 K			
	M_r (emu/g)	H_c (Oe)	M_s (emu/g)	$S = \frac{Mr}{Ms}$	M_r (emu/g)	H_c (Oe)	M_s (emu/g)	$S = \frac{Mr}{Ms}$
CFMO1	3.75	167	65.39	0.057	25.77	1388	70.18	0.367
CFMO3	4.36	159	76.35	0.057	29.66	1380	79.77	0.371
CFMO5	5.58	162	81.83	0.068	37.42	1418	84.57	0.442

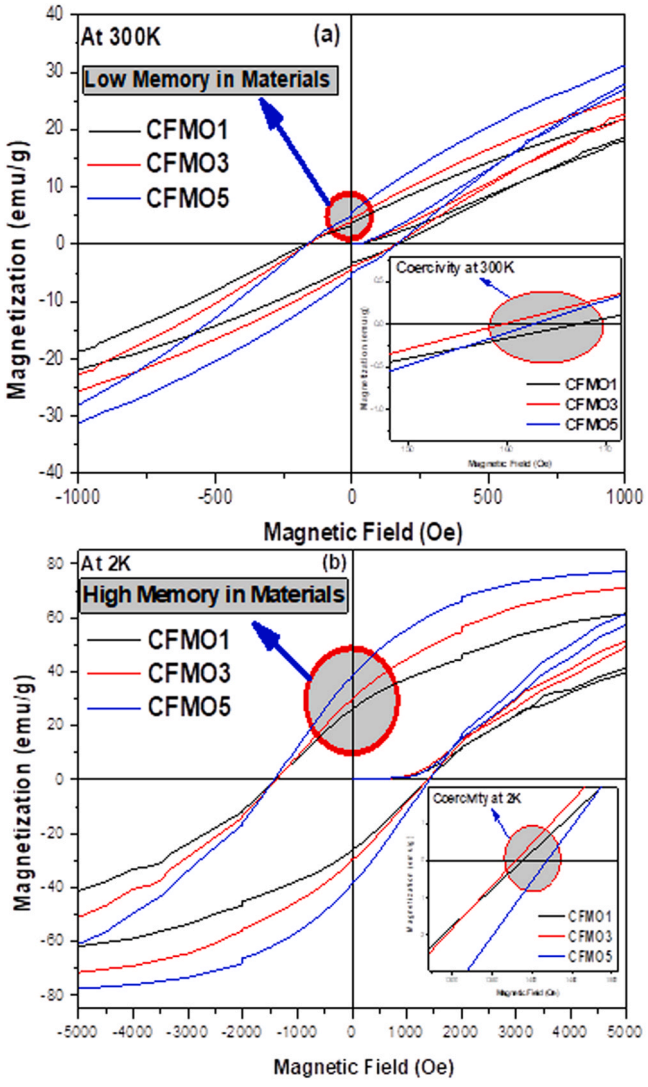

Fig. 4. Enlarge view of remenancy and coercivity values for the confirmation of magnetic memory capacity of $CoFe_{2-x}Mo_xO_4$ ceramics at (a) 300 K and (b) 2 K, respectively.

behavior of M_r, M_s, and H_c values are also the characteristics of ferrimagnetic materials [11]. Our XRD results clearly confirm the proper doping of 'Mo' in to CFO at Fe site as per the structural discussion in the above section. So it is clear that the 'Mo' is entered inside the tetrahedral site of the CFO and therefore Mo^{6+} in to the tetrahedral site will increase the overall magnetization of all samples. For the charge neutrality, at the time of Fe^{3+} to Fe^{2+} ions transformation, one of Mo^{6+} ion will transfer three Fe^{3+} in to Fe^{2+} ions. As a result of it, the magnetization will decrease at the octahedral site. Overall, we have observed the enhancement in the magnetization values with the 'Mo' concentration which is consistent with the reasoning mentioned here and in the reported literature [11].

There is a factor that much more important for the information storage purpose in the M-H hysteresis loop, i.e., coercive squareness (S*) and loop squareness, the ratio of M_r to M_s, which is labeled the remnant squareness (S) [15]. The ideal value of both S and S* (ideally close to unity) of any magnetic material decides the capability of the head to write the medium and use of digital recording media. In the present case, the value of S is minimum for CFMO compositions (~0.057–0.068) at room temperature, but drastically enhanced (~0.367–0.442) at a shallow temperature (2 K), also tabulated in Table 2 and can be seen in the Fig. 3(a-b). The enlarge view for remenancy and coercivity values are also shown in the Fig. 4(a-b) for the clear confirmation. We have obtained the maximum value of loop squareness S~0.442 for CFMO3 composition at 2 K, which can be used in information storage device applications. Although this value is not so close to unity, but much better in the case of powder

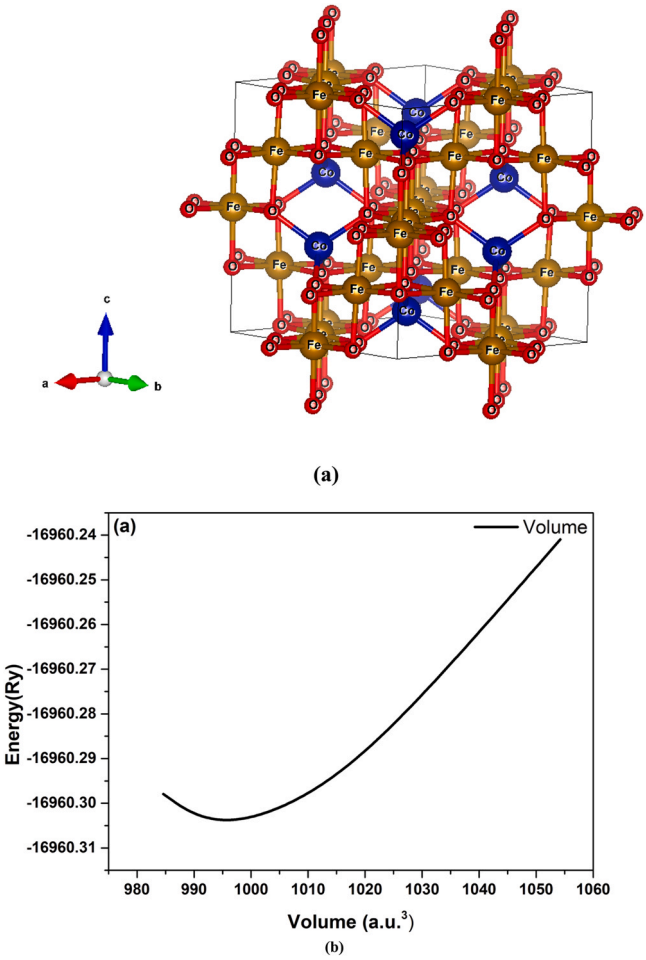

Fig. 5. (a) Optimized crystal structure for CFO and (b) optimized energy-volume curve for CFO compound under PBE-GGA exchange correlation function.

magnetic materials as reported so far [16,17]. The scope of improvement in this value after checking further with nanoparticles as well as in thin films and also can do with a higher concentration of 'Mo' type doping. We are working on this line and will try to report with further improvement soon.

Fig. 3(c) shows the zero-field cooled (ZFC) and field cooled (FC) magnetization curve of the samples at an applied field of 100 Oe in the temperature range 5–300 K. The irreversibility in ZFC and FC curves observes at blocking temperature T_B (~300 K) for all samples. Below T_B, FC, and ZFC curves start to diverge significantly, and above it, they coincide with each other for all samples. With a decrease in temperature, the ZFC curve falls rapidly below 300 K, while the FC curve becomes saturated after the initial drop for all samples. Furthermore, the increase in the amount of non-magnetic 'Mo' dopant at the Fe-site raised the FC and ZFC magnetization values in the entire temperature range. Such an increase in FC and ZFC magnetization values with 'Mo' doping may arise due to a decrease in anisotropy constant of Co^{2+} ions. It is due to the increased anisotropy constant of Co^{2+} ions in the pure cobalt ferrite hinder the samples from achieving saturation magnetization [18]. The non-magnetic 'Mo' insertion at the Fe-site enhances the saturation magnetization by reducing the anisotropy of cobalt ions in cobalt ferrite.

3.3. First principle DFT calculations

3.3.1. Computational details and crystal structure

For theoretical investigation, we have performed density functional theory (DFT) calculations on CFO compound using Wien2K code [19,20]. To study the different physical properties such as structural, electronic and magnetic, firstly CFO crystal having space group (Fd3m; S.G. No. 227) and lattice constant; a = 8.3849 Å [11,13,14] has been optimized using the Birch Murnaghan equation of states [21]. The optimized crystal structure and volume optimization curve have been displayed in Fig. 5(a,b). and the estimated lattice parameters were tabulated in Table 1. It has been observed that both the experimental (calculated from Fig. 1(a)) and theoretical lattice parameters were in good agreement to each other (Table 1). Optimized structure and lattice parameters were further used to estimate the electronic (density of states, band structure) and magnetic properties for the CFO compound.

3.3.2. Electronic (density of states and band structure) properties

To explore the electronic behaviour of the CFO compound in detail, spin polarized density of states (DOS) calculation were performed across the Fermi level. The Fermi level was set to be at 0.0 eV. Fig. 6(a-d) shows the DOS profile for the CFO compound plotted between the energy range − 9.0–7.0 eV for both the spin channel (up & dn). To gain more insight about the orbital contribution in the total DOS, DOS due to different orbital such s, p and d orbital were estimated for Co, Fe and O atoms. Fig. 6(a) represents the total-DOS profile for the CFO compound along with the total DOS due to Co, Fe and O atoms. It has been observed that there is the presence of majority of states due to Co and Fe atoms at the Fermi level along with states due to O atoms. The presence of electronic states at the Fermi level represents the metallic character of CFO compound. Individually, the partial DOS has been shown in Fig. 6(b-d) for Co, Fe and O atoms, respectively which shows that Co-3d, Fe-3d states have major contribution in total DOS near the Fermi level. Some states of Co-3d/Fe-3d also hybridize with O-2p states near the Fermi level and responsible for the resultant DOS (Fig. 6a). It has also been observed that deep inside the valence band (V.B.) from - 8.0 eV to - 3.0 eV, Co/Fe-3d states hybridize with O-2p states and results in the observed

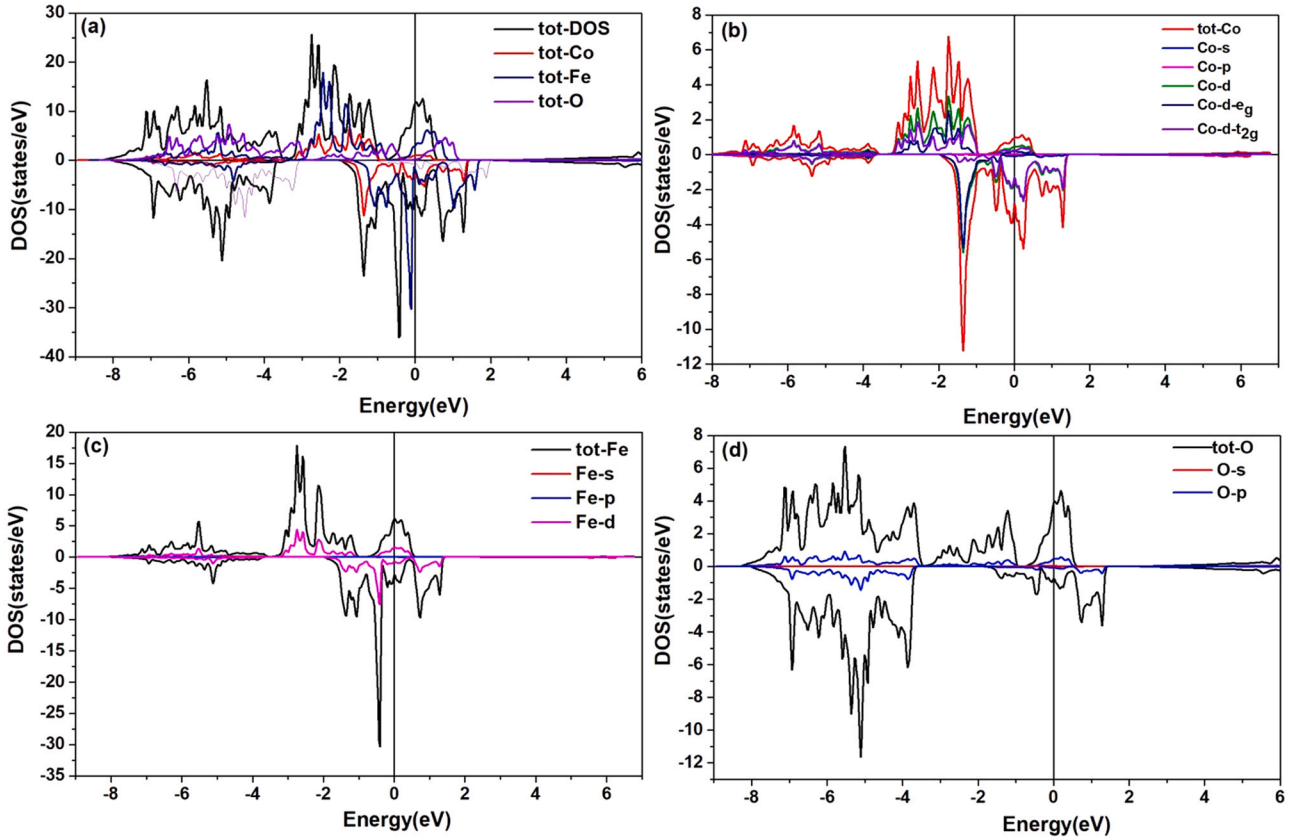

Fig. 6. (a) Estimated total-DOS profile of CFO compound along with the contribution due to Co, Fe and O atoms (b) tot-DOS due to Co atoms along with contribution due to s, p and d orbitals of Co atoms, (c) tot-DOS due to Fe atoms along with contribution due to s, p and d orbitals of Fe atoms, (d) tot-DOS due to O atoms along with contribution due to s and p orbitals of O atoms.

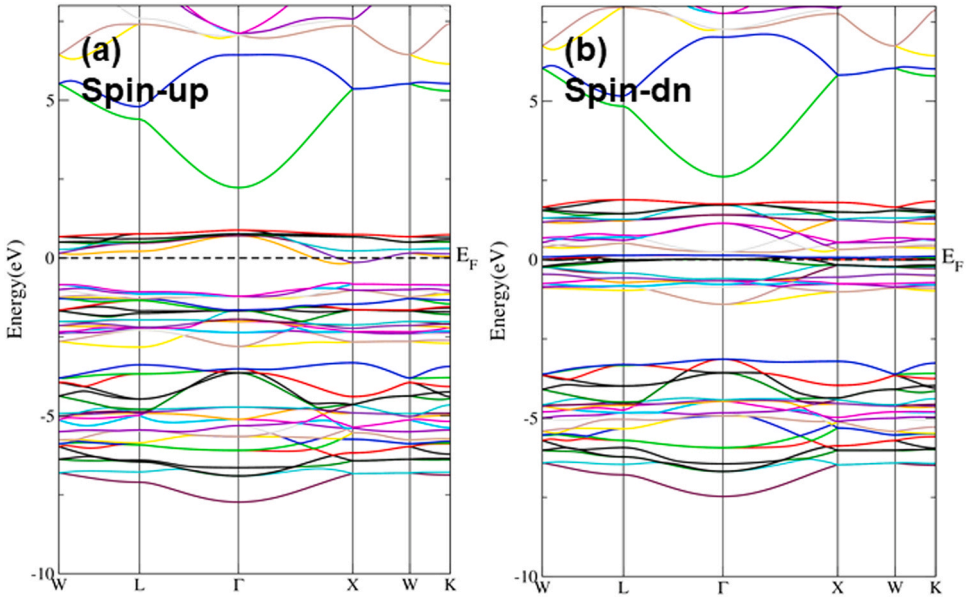

Fig. 7. Band structure profile (a) due to spin up and (b) due to spin down across the Fermi level for CFO compound.

DOS. Other Co-s, Co-p, Fe-s, Fe-p and O-s states show small contribution in the total DOS of Co, Fe and O atoms, respectively. In study, to collect more information regarding electronic behaviour, spin polarized band structure calculation has also been performed for CCMO compound. Band structure for both spin channels along with highly symmetric directions are displayed in Fig. 7(a,b). Band structure for spin up and spin down channels shows that many states are available at the Fermi level (E_F), which confirmed the metallic character of the CFO compound and well matches with the DOS profile as discussed above.

3.3.3. Magnetic properties

Magnetic moment for CFO compound has also been calculated theoretically. Obtained magnetic moment data suggests that Co (~2.3 μ_B) and Fe (~1.24 μ_B) atoms have major contribution in the magnetic moment of a cell and shows magnetic ordering of CFO compound. Little contribution has been observed in magnetic moment of a cell due to the O (0.04 μ_B) atoms. Total spin magnetic moment in a unit cell was found to be ~ 3.4 μ_B/f.u which is ~ 81.7 emu/g. Similar value of magnetization has also been observed from experimental M-H curve of CFO as discussed in the above section and well support with the present and other reported experimental findings [11,22]. Our DOS profile also represents the major contribution due to Co-3d and Fe-3d states in the TDOS.

4. Conclusions

In summary, the present analysis of $CoFe_{2-x}Mo_xO_4$ ceramics confirm the high value of information storage parameter S~0.442 in the 3%Mo doped $CoFe_2O_4$ sample at extremely low temperature (2 K). Rietveld analysis confirms the pure phase cubic crystal structure and a slight decrease in lattice parameters. Both magnetic M-H and ZFC-FC measurements confirm the enhancement in magnetic parameters and a decrease in anisotropy constant of Co^{2+} ions. In conclusion, our results provide the pure phase, enhanced magnetic parameters, and the high value of the information storage parameter in 'Mo' doped $CoFe_2O_4$ samples. In-depth investigations on enhancement in information storage and multiferroic magnetoelectric coupling in $CoFe_{2-x}Mo_xO_4$ are under progress. Our theoretical (electronic and magnetic) calculation also support with our experimental findings.

CRediT authorship contribution statement

Manish Kumar: Writing – original draft, Formal analysis. **Arvind Kumar:** DFT calculations, Writing – original draft (theoretical calculation), Formal analysis. **Abhishek Singh:** Magnetic measurments, Magnetic measurements, Formal analysis. **Subhash Sharma:** Structural, Structural investigations, Formal analysis**. Avneesh Anshul:** Formal analysis. **Prakash Chandra Sati:** Formal analysis.

Data availability

The data that support the findings of this study are available from the corresponding authors upon reasonable request.

Declaration of Competing Interest

The authors declare that they have no known competing financial interests or personal relationships that could have appeared to influence the work reported in this paper.

Acknowledgements

Authors are thankful to Central Instrument Facility (CIF), IIT(BHU), Varanasi-221005, India for XRD and SQUID measurements. Authors are also thankful to Dr. Manish Kumar Srivastava, Department of Physics, Bansthali Vidyapith, Rajasthan, India for XRD measurment. Author (M. Kumar) is thankful to University of Delhi, New Delhi for funding through Star Innovation Project (ARSD-SIP-01).

References

[1] W. Hu, N. Qin, G. Wu, Y. Lin, S. Li, D. Bao, Opportunity of spinel ferrite materials in nonvolatile memory device applications based on their resistive switching performances, J. Am. Chem. Soc. 134 (2012) 14658-61.
[2] S. Manipatruni, D.E. Nikonov, C.C. Lin, T.A. Gosavi, H. Liu, B. Prasad, Y.L. Huang, E. Bonturim, R. Ramesh, I.A. Young, Scalable energy-efficient magnetoelectric spin–orbit logic, Nature 565 (2019) 35–42.

[3] B. Li, H. Cao, J. Shao, M. Qu, J.H. Warner, Superparamagnetic Fe_3O_4 nanocrystals@ graphene composites for energy storage devices, J. Mater. Chem. 21 (2011) 5069.
[4] C. Tannous, R.L. Comstock, Springer Handbook of Electronic and Photonic Materials, (2017), https://doi.org/10.1007/978-3-319-48933-9_49
[5] R.L. Comstock, C.D. Mee, et al., Workman: data storage in rigid disks, Magnetic Storage Handbook, second ed., McGraw-Hill,, New York, 1996.
[6] R.L. Comstock, Introduction to Magnetism and Magnetic Recording, Wiley, New York, 1999.
[7] B.P. Jacob, S. Thankachan, S. Xavier, E.M. Mohammed, Dielectric behavior and AC conductivity of Tb3+ doped Ni0.4Zn0.6Fe2O4 nanoparticles, J. Alloy. Compd. 541 (2012) 29–35.
[8] B. Zhou, Y.W. Zhang, C.S. Liao, F.X. Cheng, C.H. Yan, L.Y. Chen, S.Y. Wang, Enhanced magneto-optical Kerr effects and decreased Curie temperature in Co-Mn ferrite thin films, Appl. Phys. Lett. 79 (2001) 1849–1851.
[9] Y. Melikhov, J.E. Snyder, D.C. Jiles, A.P. Ring, J.A. Paulsen, C. Lo, K.W. Dennis, Temperature dependence of magnetic anisotropy in Mn –substituted cobalt ferrite, J. Appl. Phys. 99 (2006) 08R102.
[10] N. Ranvah, Y. Melikhov, D.C. Jiles, J.E. Snyder, A.J. Moses, P.I. Williams, S.H. Song, Temperature dependence of magnetic anisotropy of Ga-substituted cobalt ferrite, J. Appl. Phys. 103 (2008) 07E506.
[11] G.D. Dwivedi, K.F. Tseng, C.L. Chan, P. Shahi, J. Lourembam, B. Chatterjee, A.K. Ghosh, H.D. Yang, S. Chatterjee, Signature of ferroelectricity in magnetically ordered Mo-doped $CoFe_2O_4$, Phys. Rev. B 82 (2010) 134428.
[12] S.D. Bhame, P.A. Joy, Effect of sintering conditions and microstructure on the magnetostrictive properties of cobalt ferrite, J. Am. Ceram. Soc. 91 (2008) 1976–1980.
[13] Z.K. Heiba, N.Y. Mostafa, O.H. Abd-Elkader, Effect of sintering conditions and microstructure on the magnetostrictive properties of cobalt ferrite, J. Magn. Magn. Mater. 368 (2014) 246–251.
[14] C. Orozco, A. Melendez, S. Manadhar, S.R. Singamaneni, K.M. Reddy, K. Gandha, I.C. Niebedim, C.V. Ramana, Effect of molybdenum incorporation on the structure and magnetic properties of cobalt ferrite, J. Phys. Chem. C 121 (2017) 25463–25471.
[15] M.L. Williams, R.L. Comstock, AIP Conf. Proc. Magn. Mater. 5 (1971) 738.
[16] E.C. Stoner, E.P. Wohlfarth, A mechanism of magnetic hysteresis in heterogeneous alloys, Philos. Trans. R. Soc. A 240 (1948) 599.
[17] J.E. Knowles, Magnetic properties of individual acicular particles, IEEE Trans. Magn. 17 (1981) 3008–3013.
[18] A.A. Khana, U. Hira, et al., Structural, magnetic and magnetocaloric properties of $CoFe_{2-x}Mo_xO_4$ ($0.0 \leq x \leq 0.3$) ferrites, Ceram. Int. 43 (2017) 7088.
[19] P. Blaha, K. Schwarz, G.H.K. Madsen, D. Kuasnicke, J. Luitz.s, Introduction to WIEN2K an Augmented Plane Wane Plus Local Orbitals Program for Calculating Crystal Properties, Vienna University of Technology, Vienna, Austria, 2001, p. 2001.
[20] S. Kumar, N. Kumar, K. Yadav, A. Kumar, R.P. Singh, DFT investigations on optoelectronic spectra and thermoelectric properties of barium cadmium disulphide ($BaCdS_2$), Optik 207 (2020) 163797.
[21] F.D. Murnaghan, The compressibility of media under extreme pressures, Proc. Natl. Acad. Sci. 244 (1944) 30–247.
[22] B.B. -Stojić, V. Jokanović, D. Milivojević, Z. Jagličić, D. Makovec, N. Jović, M. M.-Cincović, Magnetic and structural studies of CoFe2O4 nanoparticles suspended in an organic liquid, J. Nanomater. 741036 (2013) 1–9.